Hindawi
International Journal of Photoenergy
Volume 2017, Article ID 2929473, 8 pages
https://doi.org/10.1155/2017/2929473

Research Article

Experimental Investigation on Thermal Management of Electric Vehicle Battery Module with Paraffin/Expanded Graphite Composite Phase Change Material

Jiangyun Zhang, Xinxi Li, Fengqi He, Jieshan He, Zhaoda Zhong, and Guoqing Zhang

School of Materials and Energy, Guangdong University of Technology, Guangzhou, Guangdong 510006, China

Correspondence should be addressed to Xinxi Li; pkdlxx@163.com

Received 5 September 2017; Revised 31 October 2017; Accepted 19 November 2017; Published 31 December 2017

Academic Editor: Hamidreza Shabgard

The temperature has to be controlled adequately to maintain the electric vehicles (EVs) within a safety range. Using paraffin as the heat dissipation source to control the temperature rise is developed. And the expanded graphite (EG) is applied to improve the thermal conductivity. In this study, the paraffin and EG composite phase change material (PCM) was prepared and characterized. And then, the composite PCM have been applied in the 42110 $LiFePO_4$ battery module (48 V/10 Ah) for experimental research. Different discharge rate and pulse experiments were carried out at various working conditions, including room temperature (25°C), high temperature (35°C), and low temperature (−20°C). Furthermore, in order to obtain the practical loading test data, a battery pack with the similar specifications by 2S*2P with PCM-based modules were installed in the EVs for various practical road experiments including the flat ground, 5°, 10°, and 20° slope. Testing results indicated that the PCM cooling system can control the peak temperature under 42°C and balance the maximum temperature difference within 5°C. Even in extreme high-discharge pulse current process, peak temperature can be controlled within 50°C. The aforementioned results exhibit that PCM cooling in battery thermal management has promising advantages over traditional air cooling.

1. Introduction

EVs have received universal eyes owing to their unique advantages over traditional vehicles in energy efficiency and emission reduction [1–3]. The temperature and its distribution have essential effects on the battery properties [4–6]. Such overheating and inhomogeneous temperature distribution frequently result in the module's premature failure earlier and life span degradation during practical operation process [7–9]. Especially in harsh working conditions, catastrophic destruction, such as fire and explosion, even thermal runway will occur [10–12]. It is well known that the max temperature of cells must be strictly controlled within 55°C. Also, the ΔT must be maintained below 5°C by means of effective thermal management systems [13, 14] .Therefore, selecting an appropriate heat dissipation system is of critical importance for power battery modules [15, 16]. At present, traditional air cooling [17–19] cannot transfer the heat generated from batteries quickly with the increasing module capacity and specifications. Although the liquid cooling [20, 21] method has a better heat dissipation effect, some disadvantages include complicated system, difficult maintenance, and high cost. In recent years, a novel thermal management with the PCM cooling system was proposed as an ideal substitute to the abovementioned traditional patterns [22–24].

PCM cooling technology is able to maintain the operating temperature of cells at a relatively constant temperature range, absorbing/releasing abundant heat during change of phase. The solution can make the temperature within the optimal range, managing uniform temperature distribution, especially in the extreme environment. Zhao et al. [25] summarized different kinds of thermal management methods and obtained the conclusion that PCM heat dissipation

technology is very promising for battery management systems. Karimi et al. [26] had an experimental study of a cylindrical lithium-ion battery thermal management using PCM composites and found that the metal matrix-PCM composite decreases the max ΔT between battery surface and PCM composite by up to 70%. The thermal management with $LiFePO_4$ battery pack at high temperature using a composite of PCMs and aluminum wire mesh plates was investigated by Azizi and Sadrameli [27], which displayed that the maximum surface temperature of battery was reduced by 19%, 21%, and 26% at 1C, 2C, and 3C discharge rate, respectively. Wilke et al. [27] had an experiment about preventing thermal runaway propagation in lithium-ion battery packs using a phase change composite material and got that the use of PCC (phase change composite) lowers the max temperature experienced by neighboring cells by 60°C or more. As a widely used organic phase change material, paraffin has many advantages, including high-phase change latent heat, wide melting point range, stable thermal performance, easy molding in solid state, generally not disappear phase separation phenomenon, and low corrosion and cost. Nevertheless, the thermal performance of low conductivity restricts the use of PCM-based cooling systems in subsequent application. In this paper, as a porous high thermal conductive material, expanded graphite is used to improve the thermal conductivity of materials. At present, most research about various battery thermal management systems are limited to the laboratory experiments under different working conditions, few practical loading tests are conducted according to the real driving road operation.

In this paper, a completely novel PCM-based cooling system, for 42110 cylindrical $LiFePO_4$ battery pack (96 V/20 Ah), has been introduced and developed herein. The battery pack made-up of four battery modules (48 V/10 Ah) by 2 series 2 parallel with the same technical parameters was carried out for practical pure electric vehicle (EV) loading experiments. The EV, with 96 V/150 Ah lead-acid power batteries, was assembled into lithium-ion battery pack (96 V/20 Ah). Various road conditions were conducted for evaluating the heat dissipation and temperature uniform distribution, including flat ground, 5-degree, 10-degree, and 20-degree slope. The composite PCM was prepared and its thermophysical performance was tested, including the thermal conductivity coefficient, latent heat, and thermalgravimetric (TG). Relevant experimental results indicated that cooling effect of PCM heat dissipation technology had more advantages over traditional air natural cooled, which showed PCM cooling system had a bright future for thermal management in the power battery module.

2. Experimental Setup

2.1. Composite Material Preparation and Characterization. Composite PCM was obtained by a physically mixing method. Firstly, industrial-grade paraffin (melting point from 35 to 40°C) was used. Expandable graphite with an average particle size (150 μm) and expansion ratio (220 mL g^{-1}) was obtained from Qingdao Bai Xing Graphite Co., Ltd. Secondly, EG was obtained by heating the expandable graphite at 800°C for 60 s in a muffle furnace. PA was heated to 80°C. EG was added to the completely melting PA at a mass ratio of 4 : 1 with continuous mechanical stirring. Finally, through the hot-compaction process in a mold, a composite PCM module was fabricated with an overall dimension of 228.25 mm (length) × 142.34 mm (width) × 110 mm (height). The 42110 cylindrical cells were inserted into the 15 holes uniformly distributed on the PCM module, each with a diameter of 42.5 mm and height of 110 mm. The construction and fabrication of the PCM module were provided in Figure 1. Detailed preparation process of the composite material was described in our group previous research [28].

The microstructure of the composite PCMs was tested by a scanning electron microscope (SEM, Hitachi S-3400 N, Japan). The thermal conductivity was observed by an LFA447 NanoFlash™ system (range 0.1–2000 $W \cdot m^{-1} \cdot k^{-1}$, accuracy ±5%, repeatability ±3%). The latent heat was measured using a Differential Scanning Calorimeter (HS-DSC-101B, HESON Instrument Inc., Shanghai).

2.2. Battery Module Construction. Figure 2 described the battery module assemble process. There were 15 holes with a diameter of 42.3 mm on the composite PCM module, in which 15 commercial 42110 Li-ion batteries (3.2 V/10 Ah) with symmetric distribution of T-type thermocouples were placed (layout of thermocouples were showed in Figure 3). All the cells were electrically connected in 15S1P configuration electric connection (15 cells in series and 1 string in parallel) by nickel pieces. Finally, the module technical parameters were shown in Table 1.

Technical specifications of the power battery module are provided in Table 1.

2.3. Design of the Experiment System. The experiment facilities are summarized in Figure 3. The constant-current sources (YK-AD12015, 120 V/15A, 1800 W) were used for module charging. DC electric load (M9718, 240 V/150A, 6000 W) was provided for constant-current discharging and acquiring current and voltage data during the discharge process. The temperature inspection instrument was used for collecting temperature data real-time.

2.4. Module Laboratory Testing. The PCM battery module was tested at a constant room temperature of 29°C. T-type thermocouples (OMEGA type SMPW-T-M) were placed inside the module to measure the battery surface temperature. During the experiment, the battery module was subjected to the following charge protocol: galvanostatic mode at 0.5C rate with a voltage cutoff limit of 59.0 V and then a potentiostatic mode until the current drops to 0A. After the charging process, adequate equilibration time was left for cooling the module to ambient temperature. Subsequently, the battery module was discharged at specified rates including 2.0C and 4.5C, respectively. Meanwhile, pulse experiment with high discharge current was conducted.

2.5. Pack Loading Testing. A battery pack (96 V/20 Ah) included one as-assembled PCM module and three air cooling modules in 2 series ∗ 2 parallel with the same specifications. Four modules were placed in symmetrical

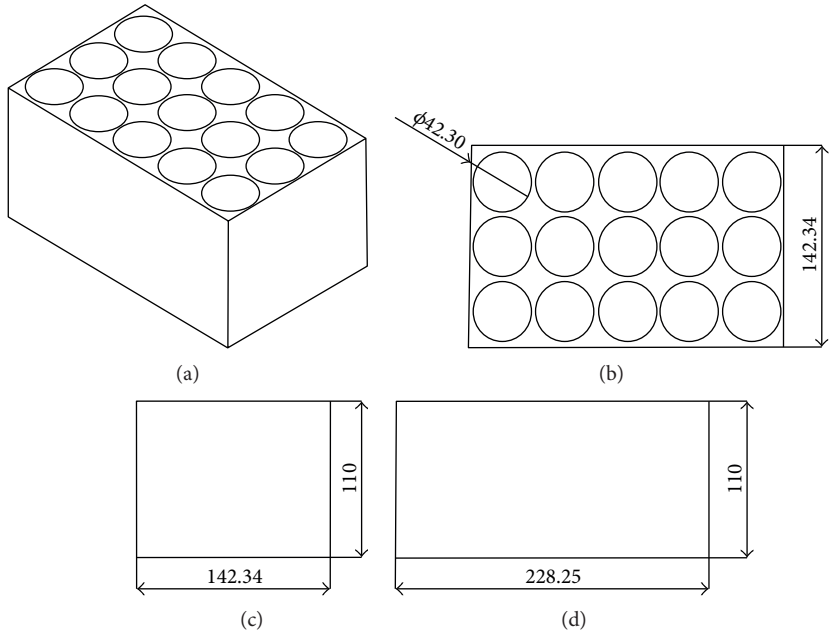

Figure 1: The battery module sizes with PCM. (a) The whole structure: (b) top view, (c) left view, and (d) front view.

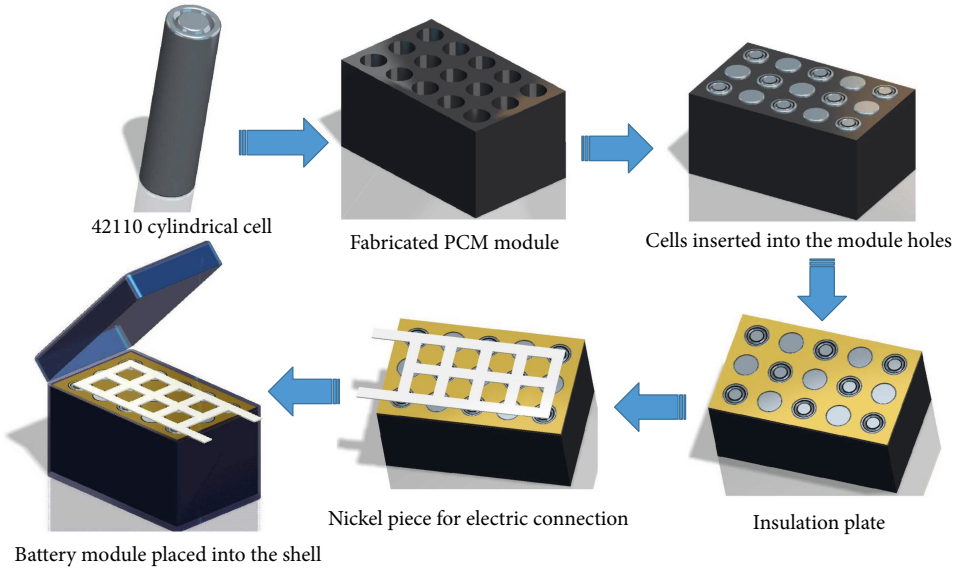

Figure 2: The battery module assembly process.

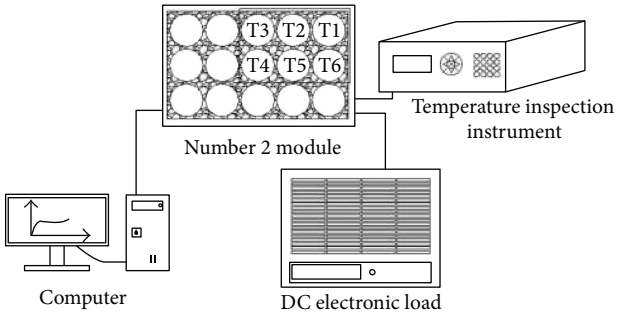

Figure 3: The sketch measurement experiment systems of battery module with PCM cooling.

Table 1: Battery module specifications.

Name	Parameters
Cell type	IFR42110LiFePO$_4$
Module nominal voltage (V)	48
Module nominal capacity (Ah)	10
Max discharge current (A)	50
Max charge current (A)	10
Operating temperature range (°C)	−20~60
Charging temperature range (°C)	0~45

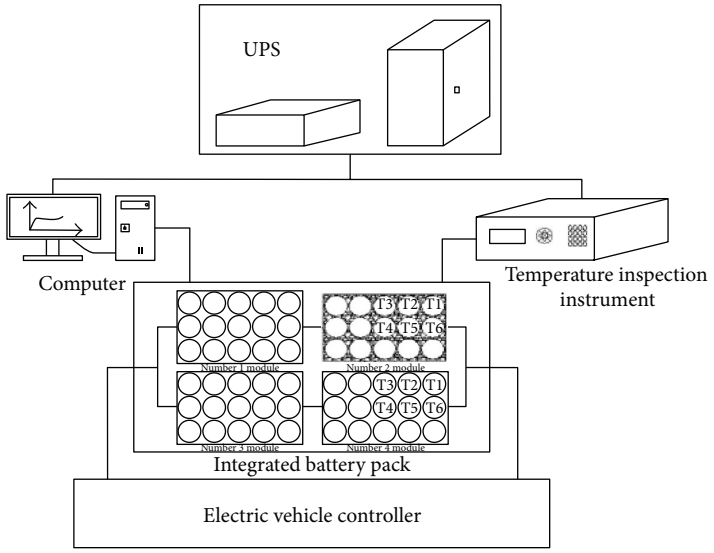

Figure 4: An illustration of the loading test setup.

distribution; therefore, one-quarter of both the PCM and air-cooled module were selected for collecting the temperature real-time. The pack was connected with the electric vehicle controller through 175A 600 V industrial plugs. Uninterruptible power supply (UPS) was used for providing the electric power to the temperature inspection instrument and the computer. The UPS with two lead-acid (12 V/38 Ah) battery modules in series was backup style which means that the host and its power are connected separately by communication signal wires. The loading test experiment setup scheme was shown in Figure 4. (Number 1, number 3, and number 4 battery modules designed with air-cooled scheme, number 2 module designed with PCM-based cooling, all with the same technical parameters. T4 stood for the cell temperature located in the module middle, and T1 represented the cell temperature located in the module edge.)

3. Results and Discussion

3.1. Characterization of Composite PCMs. DSC results of pure paraffin (PA) and paraffin/EG composite were shown in Figure 5. After adding EG, the latent heat of paraffin/EG composite decreased from 200.64 J/g to 147.61 J/g. In addition, the melting points of PA and PA/EG composite were 41.5 and 40.4°C, respectively, which is consistent with the melting point variations tendency of PA/EG composite proposed by Radhakrishnan and Gubbins [29, 30].

Thermal conductivity coefficient of composite ranging from 35°C to 50°C with 5°C internal was shown in Figure 6. Testing data indicated that the thermal conductivity came to the highest at 40°C (nearly close to the melting point 41.5°C), which was 3.084 $W \cdot m^{-1} \cdot k^{-1}$, almost 12 times larger than that of pure paraffin (0.26 $W \cdot m^{-1} \cdot k^{-1}$). Above results could be owed to the EG high thermal conductivity. Figure 7 compared the mass changing trend with the temperature of pure PA and PA/EG composite named TG curves. Linear slope of PA was greatly higher than that of PA/EG composite.

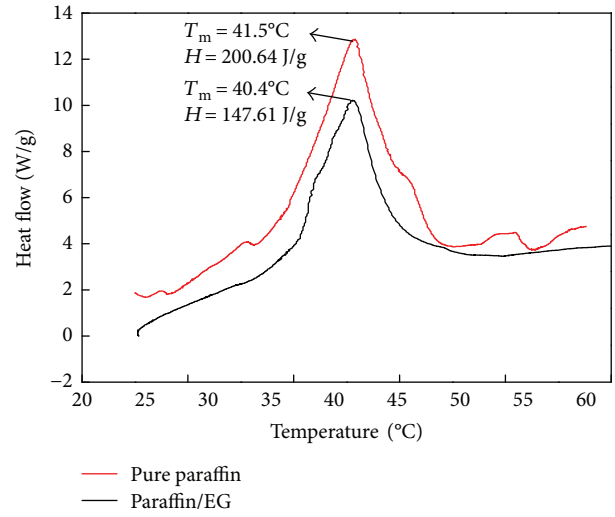

Figure 5: The comparison of latent heat between pure PA and PA/EG composite PCM.

The PA volatilization temperature was 100°C (PA nearly 100% volatilized), and the composite was 250°C (PA nearly 100% volatilized). The addition of EG can effectively delayed the paraffin volatilizing temperature and make the TG curve more smooth. Therefore, expanded graphite not only obviously improves the thermal stability but also decrease the volatilizing rate effectively.

3.2. Comparison of Heat Dissipation Performance

3.2.1. Constant-Current Discharge Test Results of PCM Cooling Module. The battery module was discharged at 2.0C and 4.5C, respectively, under room temperature condition (29°C). Comparisons of the experimental data were shown in Figure 8. Meanwhile, the module was tested at

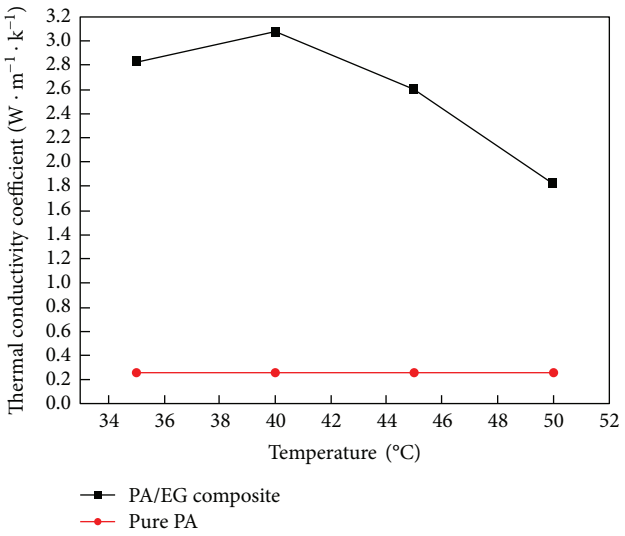

Figure 6: Thermal conductivity analysis between pure PA and PA/EG composite PCM.

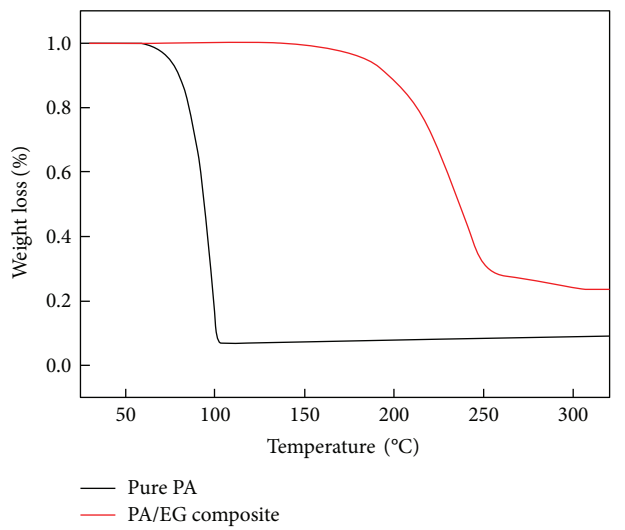

Figure 7: TG curves of pure PA and PA/EG composite PCM.

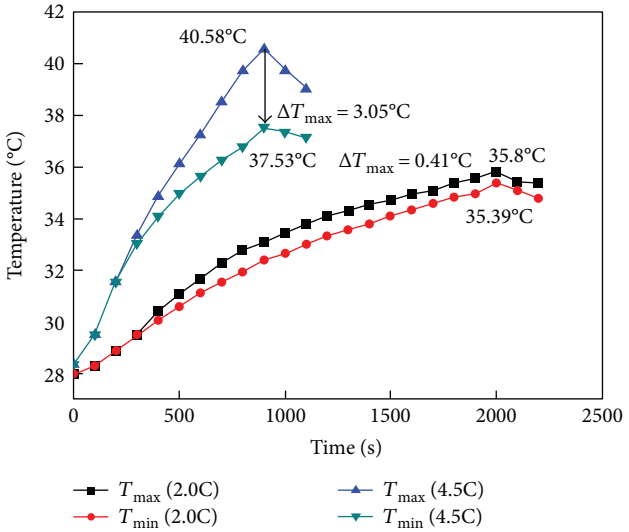

Figure 8: The T_{max} and T_{min} comparisons of battery module with PCM cooling at 2C and 4.5C, respectively (T_{max} meant number 4 cell; T_{min} meant number 1 cell).

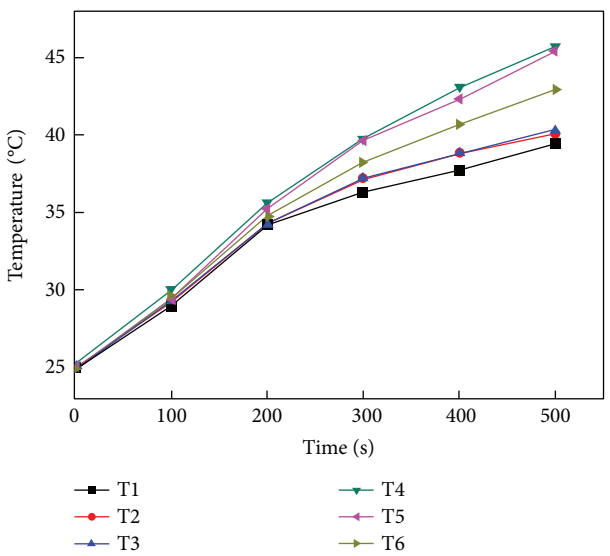

Figure 9: Temperature test results of pulse discharge experiments.

different discharge rates under low temperature (−20°C) and relatively high temperature (35°C) condition, respectively.

Figure 8 indicated number 4 cell temperature at 2.0C and 4.5C discharge rate came to 35.8 and 40.58°C, respectively, which indicated the core temperature came to the highest. Additionally, the above maximum temperature value is nearly closed to the PCM melting point and the max ΔT for 2.0C and 4.5C is 0.41°C and 3.05°C, respectively (which is significantly less than 5°C), which showed more excellent temperature uniform distribution. At 3C discharge rate, the room temperature, high temperature, and low temperature reached 37.61°C, 38.23°C, and 32.38°C, respectively, which revealed that high temperature was higher at 1.64% and 18.06% compared to that of the room and low-temperature condition. The test data indicated that PCM cooling system can control the max temperature well below 42°C and accompany with excellent distribution, which means that the peak ΔT can be managed within 5°C. Therefore, the PCM cooling effect can satisfy the heat dissipation requirement, while maintaining the max temperature and keeping the temperature difference within the safety range.

3.2.2. Pulse Test with High Discharge Current. Pulse experiments were conducted in order to test the PCM cooling battery module, accompanied with the temperature instantaneous change and discharge performance. Detailed test stage was as follows: (a) charge state: galvanostatic mode at 0.5C rate with a voltage cutoff limit of 59.0 V and then a potentiostatic mode until the current descended to 0A. (b) Hold stage: 1.5 h. (c) Pulse discharge stage: The module was discharged under a constant current of 10.0C for 10 s, then hold for 10s, next discharge at 4.5C for 5 s, then the rest for

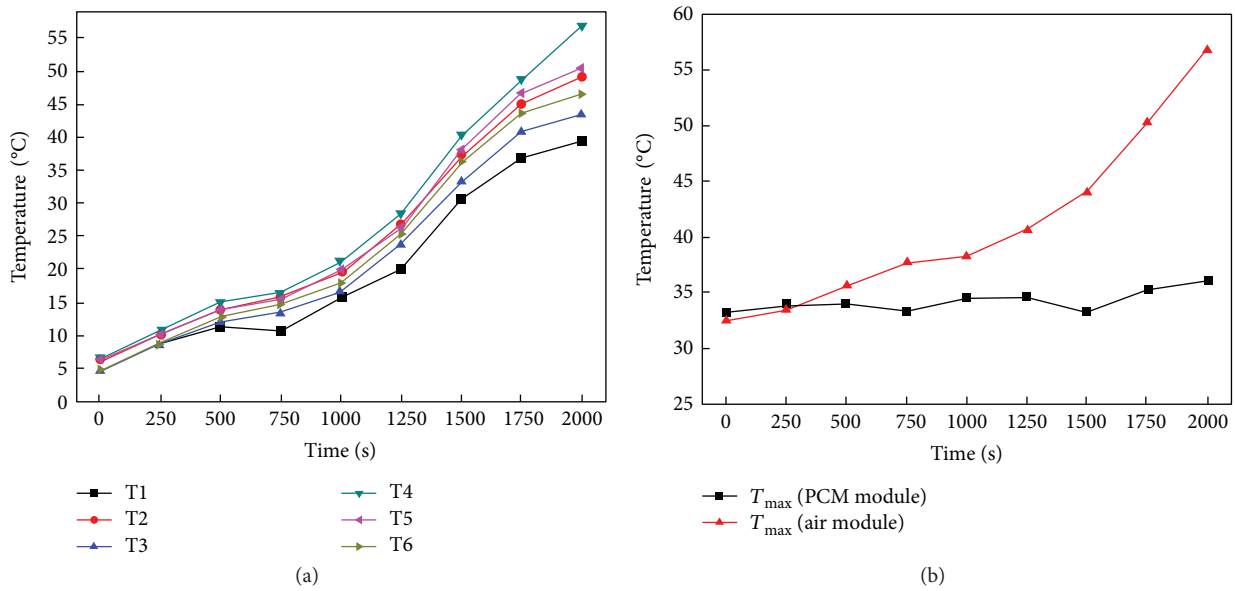

Figure 10: Pack testing results on the flat ground. (a) Temperature curve of the air-cooled module. (b) The T_{max} comparison of test data between the air cooling module and PCM cooling module. (T_{max} meant number 4 cell).

Table 2: Comparison of experimental results.

Road condition	T_{max} (°C) (PCM)	T_{min} (°C) (PCM)	ΔT_{max} (°C) (PCM)	T_{max} (°C) (air-cooled)	T_{min} (°C) (air-cooled)	ΔT_{max} (°C) (air-cooled)
Ground	35.1	31.8	3.3	56.8	49.3	7.5
5°slope	36.87	33.75	3.12	39.6	33.5	6.2
10°slope	36.38	35.1	1.28	42.25	36.2	6.05
20°slope	36.5	34.5	2.0	44.8	38	6.8

10 s. All the test period was 475 s. (d) Hold stage: 1.0 h. Test data was present in Figure 9.

Figure 9 Indicates the max temperature (number 4 cell) of the module core location reaches 45.65°C which is managed within 50°C in extreme instantaneous high discharge rate condition owing to PCM cooling technology participation. The minimum data (number 1 cell) of the module edge location reached to 39.44°C. Even discharged under the 10.0C high current pulse condition, the max temperature can still be controlled within the 50°C, which showed superior temperature instantaneous change ability.

3.3. Loading Test Results and Discussion

3.3.1. Driving Test Results on the Ground. One-quarter of the module was regarded as the research object according to the symmetry principle. Experiments were processed on the fixed road A, and the results were taken from the average of three-times experiments. Air-cooled module temperature data was obtained in Figure 10(a). The comparison of the max temperature curves between air-cooled and PCM cooling modules was displayed in Figure 10(b).

In Figure 10(b), the red curve indicated the max temperature with pure air cooling module comes to 56.8°C, which presented a rapidly increasing tendency. In contrast, the black curve revealed the max temperature with the PCM cooling module can reach to 36°C and decreases by 57.7%, which displayed a slowly increasing tendency. Therefore, the battery module with the PCM cooling system can improve the thermal management effectively.

3.3.2. Data Analysis on Different Road Conditions. Comparisons of test results on different road conditions are shown in Table 2.

Table 2 shows that peak temperature and its difference of the air cooling module is always higher than that of the PCM cooling module. The max temperature of the air-cooling module on the ground reaches 56.8°C which has exceeded 55°C with 7.5°C peak ΔT and will have a heavy influence on the battery electric chemistry performance. Therefore, the cooling effect of the PCM system is far superior that of air cooling.

4. Conclusions

The paraffin and EG composite PCM were applied to battery modules for thermal management in this study. Thermal performance, including latent heat, thermal conductivity, and TG curves of PA/EG composite were carried out, respectively. The 42110 $LiFePO_4$ battery module (48 V/10 Ah) is investigated at different discharge rates under

various conditions. Simultaneously, practical loading work under different road conditions was processed. The conclusions were summarized based on the experimental results as follows:

(1) The composite thermal conductivity reached 3.084 $W \cdot m^{-1} \cdot k^{-1}$ at 40°C, as the max value, which was nearly 12 times higher than that of PA. Also, the composite volatilization temperature was delayed to 250°C with more smooth TG curve owing to EG participation and the thermal stability was greatly improved. The latent heat of the PA/EG composite came to 147.61 J/g, which was 35.9% lower than that of PA. Also, the melting point of PA/EG composite showed a decreasing tendency.

(2) Peak temperature gradually increased with the rise of discharge rates under each condition. On one hand, the results showed that the max temperature and its peak difference of the module could be controlled within 42°C and 5°C under constant-current discharge condition, respectively. On the other hand, even in extreme 10.0C pulse discharge rate, peak temperature is always controlled within 50°C which can meet the heat dissipation demand. The heat dissipation was greatly improved by the PCM cooling system which exhibited excellent temperature controlling and temperature balance ability.

(3) Loading test data showed the max temperature and its peak difference of PCM cooling were always lower than that of the air-cooling module, which revealed that the PCM cooling can exhibit excellent thermal management for battery modules.

Conflicts of Interest

The authors declare that there are no conflicts of interest regarding the publication of this paper. The authors confirm that the mentioned received funding in the Acknowledgments section did not lead to any conflict of interests regarding the publication of this manuscript.

Acknowledgments

This work is supported by the Science and Technology Planning Project of Guangdong Province, China (2014B0 10128001), South Wisdom Valley Innovative Research Team Program (2015CXTD07), Scientific and Technological Project of Administration of Quality and Technology Supervision of Guangdong Province (2015PJ03), Science and Technology Application Research and Development Projects of Guangdong Province, China (2015B010135010), and Science and Technology Plan Projects of Guangdong Province, China (2016B090918015).

References

[1] Q. C. Wang, Z. H. Rao, Y. T. Huo, and S. F. Wang, "Thermal performance of phase change material/oscillating heat pipe-based battery thermal management system," *International Journal of Thermal Sciences*, vol. 102, pp. 9–16, 2016.

[2] W. X. Wu, X. Q. Yang, G. Q. Zhang, K. Chen, and S. F. Wang, "Experimental investigation on the thermal performance of heat pipe-assisted phase change material based battery thermal management system," *Energy Conversion and Management*, vol. 138, pp. 486–492, 2017.

[3] T. Yuksel, S. Litster, V. Viswanathan, and J. J. Michalek, "Plug-in hybrid electric vehicle $LiFePO_4$ battery life implications of thermal management, driving conditions, and regional climate," *Journal of Power Sources*, vol. 338, pp. 49–64, 2017.

[4] F. C. Wu and Z. H. Rao, "The lattice Boltzmann investigation of natural convection for nanofluid based battery thermal management," *Journal of Applied Thermal Engineering*, vol. 115, pp. 659–669, 2017.

[5] S. Shi, Y. Xie, M. Li et al., "Non-steady experimental investigation on an integrated thermal management system for power battery with phase change materials," *Energy Conversion and Management*, vol. 138, pp. 84–96, 2017.

[6] A. Hussain, C. Y. Tso, and C. Y. Chao, "Experimental investigation of a passive thermal management system for high-powered lithium ion batteries using nickel foam-paraffin composite," *Energy*, vol. 115, Part 1, pp. 209–218, 2016.

[7] D. Chen, J. Jiang, G. H. Kim, C. Yang, and A. Pesaran, "Comparison of different cooling methods for lithium ion battery cells," *Applied Thermal Engineering*, vol. 94, pp. 846–854, 2016.

[8] S. Basu, K. S. Hariharan, S. M. Kolake, T. Song, D. K. Sohn, and T. Yeo, "Coupled electrochemical thermal modeling of a novel Li-ion battery pack thermal management system," *Applied Energy*, vol. 181, pp. 1–13, 2016.

[9] Z. Qian, Y. Li, and Z. Rao, "Thermal performance of lithium-ion battery thermal management system by using mini-channel cooling," *Energy Conversion and Management*, vol. 126, pp. 622–631, 2016.

[10] J. Qu, J. T. Zhao, and Z. H. Rao, "Experimental investigation on the thermal performance of three-dimensional oscillating heat pipe," *International Journal of Heat and Mass Transfer*, vol. 109, pp. 589–600, 2017.

[11] C. Z. Liu, Z. Y. Ma, J. T. Wang, Y. M. Li, and Z. H. Rao, "Experimental research on flow and heat transfer characteristics of latent functional thermal fluid with microencapsulated phase change materials," *International Journal of Heat and Mass Transfer*, vol. 115, Part A, pp. 737–742, 2017.

[12] Z. H. Rao, Z. Qian, Y. Kuang, and Y. M. Li, "Thermal performance of liquid cooling based thermal management system for cylindrical lithium-ion battery module with variable contact surface," *Applied Thermal Engineering*, vol. 123, pp. 1514–1522, 2017.

[13] Y. Lv, X. Yang, X. Li, G. Zhang, Z. Wang, and C. Yang, "Experimental study on a novel battery thermal management technology based on low density polyethylene-enhanced composite PCMs coupled with low fins," *Applied Energy*, vol. 178, pp. 376–382, 2016.

[14] M. Alipanah and X. Li, "Numerical studies of lithium-ion battery thermal management systems using phase change materials and metal foams," *International Journal of Heat and Mass Transfer*, vol. 102, pp. 1159–1168, 2016.

[15] C. Zheng, F. Geng, and Z. Rao, "Proton mobility and thermal conductivities of fuel cell polymer membranes: molecular dynamics simulation," *Computational Materials Science*, vol. 132, pp. 55–61, 2017.

[16] S. K. Mohammadian, S. M. Rassoulinejad-Mousavi, and Y. Zhang, "Thermal management improvement of an air-cooled high-power lithium-ion battery by embedding metal foam," *Journal of Power Sources*, vol. 296, pp. 305–313, 2015.

[17] Z. Lu, X. Z. Meng, L. C. Wei, W. Y. Hu, L. Y. Zhang, and L. W. Jin, "Thermal management of densely-packed EV battery with forced air cooling strategies," *Energy Procedia*, vol. 88, pp. 682–688, 2016.

[18] L. H. Saw, Y. Ye, A. A. Tay, W. T. Chong, S. H. Kuan, and M. C. Yew, "Computational fluid dynamic and thermal analysis of lithium-ion battery pack with air-cooling," *Applied Energy*, vol. 177, pp. 783–792, 2016.

[19] W. Tong, K. Somasundaram, E. Birgersson, A. S. Mujumdar, and C. Yap, "Thermo-electrochemical model for forced convection air cooling of a lithium-ion battery module," *Applied Thermal Engineering*, vol. 99, pp. 672–682, 2016.

[20] X. H. Yang, S. C. Tan, and J. Liu, "Thermal management of Li-ion battery with liquid metal," *Energy Conversion and Management*, vol. 117, pp. 577–585, 2016.

[21] Y. Azizi and S. M. Sadrameli, "Thermal management of a $LiFePO_4$ battery pack at high temperature environment using a composite of phase change materials and aluminum wire mesh plates," *Energy Conversion and Management*, vol. 128, pp. 294–302, 2016.

[22] W. Wu, G. Zhang, X. Ke, X. Yang, Z. Wang, and C. Liu, "Preparation and thermal conductivity enhancement of composite phase change materials for electronic thermal management," *Energy Conversion and Management*, vol. 101, pp. 278–284, 2015.

[23] T. Nomura, C. Zhu, S. Nan, K. Tabuchi, S. Wang, and T. Akiyama, "High thermal conductivity phase change composite with a metal-stabilized carbon-fiber network," *Applied Energy*, vol. 179, pp. 1–6, 2016.

[24] C. J. Lan, J. Xu, Y. Qiao, and Y. B. Ma, "Thermal management for high power lithium-ion battery by minichannel aluminum tubes," *Applied Thermal Engineering*, vol. 101, pp. 284–292, 2016.

[25] J. T. Zhao, P. Z. Lv, and Z. H. Rao, "Experimental study on the thermal management performance of phase change material coupled with heat pipe for cylindrical power battery pack," *Experimental Thermal and Fluid Science*, vol. 82, pp. 182–188, 2017.

[26] G. Karimi, M. Azizi, and A. Babapoor, "Experimental study of a cylindrical lithium ion battery thermal management using phase change material composites," *Journal of Energy Storage*, vol. 8, pp. 168–174, 2016.

[27] S. Wilke, B. Schweitzer, S. Khateeb, and S. Al-Hallaj, "Preventing thermal runaway propagation in lithium ion battery packs using a phase change composite material: an experimental study," *Journal of Power Sources*, vol. 340, pp. 51–59, 2017.

[28] W. X. Wu, X. Q. Yang, and G. Q. Zhang, "An experimental study of thermal management system using copper mesh-enhanced composite phase change materials for power battery pack," *Energy*, vol. 113, pp. 909–916, 2016.

[29] R. Radhakrishnan and K. E. Gubbins, "Free energy studies of freezing in slit pores: an order-parameter approach using Monte Carlo simulation," *Molecular Physics*, vol. 96, no. 8, pp. 1249–1267, 1999.

[30] R. Radhakrishnan, K. E. Gubbins, A. Watanabe, and K. Kaneko, "Freezing of simple fluids in microporous activated carbon fibers: comparison of simulation and experiment," *Journal of Chemical Physics*, vol. 111, no. 19, pp. 9058–9067, 1999.